



## Metal-organic framework DUT-67 (Zr) for adsorptive removal of trace $\text{Hg}^{2+}$ and $\text{CH}_3\text{Hg}^+$ in water

Sha Chen, Fan Feng, Sumei Li, Xiao-Xin Li & Lun Shu

To cite this article: Sha Chen, Fan Feng, Sumei Li, Xiao-Xin Li & Lun Shu (2018) Metal-organic framework DUT-67 (Zr) for adsorptive removal of trace  $\text{Hg}^{2+}$  and  $\text{CH}_3\text{Hg}^+$  in water, Chemical Speciation & Bioavailability, 30:1, 99-106, DOI: [10.1080/09542299.2018.1509020](https://doi.org/10.1080/09542299.2018.1509020)

To link to this article: <https://doi.org/10.1080/09542299.2018.1509020>



© 2018 The Author(s). Published by Informa UK Limited, trading as Taylor & Francis Group.



Published online: 21 Aug 2018.



Submit your article to this journal [↗](#)



Article views: 1856



View related articles [↗](#)



View Crossmark data [↗](#)



Citing articles: 12 View citing articles [↗](#)

# Metal-organic framework DUT-67 (Zr) for adsorptive removal of trace $\text{Hg}^{2+}$ and $\text{CH}_3\text{Hg}^+$ in water

Sha Chen<sup>a</sup>, Fan Feng<sup>a</sup>, Sumei Li<sup>a</sup>, Xiao-Xin Li<sup>a</sup> and Lun Shu<sup>b</sup>

<sup>a</sup>Key Laboratory of Beijing on Regional Air Pollution Control, College of Environmental and Energy Engineering, Beijing University of Technology, Beijing, PR China; <sup>b</sup>Beijing Key Laboratory for Green Catalysis and Separation and Department of Chemistry and Chemical Engineering, College of Environmental and Energy Engineering, Beijing University of Technology, Beijing, PR China

## ABSTRACT

A Zr-based stable metal-organic frameworks DUT-67 (Zr) was successfully synthesized as an adsorbent to remove trace mercury and methylmercury ions in aqueous solution. The removal efficiency of 90% and 55% of  $\text{Hg}^{2+}$  and  $\text{CH}_3\text{Hg}^+$  was respectively achieved at pH 6 and 55°C. The S in thiophene has a relatively weak adsorption capacity for mercury and there could be the slight  $\pi$ -complexation between thiophene ring of DUT-67 (Zr) and  $\text{Hg}^{2+}$  besides physical adsorption, while there only was physical adsorption between DUT-67 (Zr) and  $\text{CH}_3\text{Hg}^+$ . The developed methods were applied to remove trace  $\text{Hg}^{2+}$  and  $\text{CH}_3\text{Hg}^+$  in the real water samples, and the removal efficiency was from 69% to 90% and from 30% to 77% respectively; when the concentrations of  $\text{Hg}^{2+}$  was lower than  $20 \mu\text{g L}^{-1}$  in the samples, the remaining mercury concentration was lower than  $1 \mu\text{g L}^{-1}$ , which can meet the standard of the World Health Organization.

## ARTICLE HISTORY

Received 12 June 2018  
Accepted 31 July 2018

## KEYWORDS

Metal organic framework;  
mercury ions;  
methylmercury ions;  
adsorption

## 1. Introduction

Mercury is one of toxic heavy metal pollutants because it seriously damages to the human body [1,2]. With the implementation of the Minamata Convention, people increasingly concern about its hazard and the control of the global mercury emission becoming an emergency [3]. In aqueous solution, mercury exists in various species, such as inorganic mercury and organomercury, and its toxicity and bioavailability mainly depend on its different chemical forms [4]. Among them, mercury with oxidation state 2 valence can easily penetrate biological membranes and cause serious kidney, digestive, endocrine and central nervous system complications [5]. And the most toxic form of organomercury is methylmercury because of its bio-accumulation and concentration with food chains and it consequently causes permanent damage to the nervous systems and brains of human being [6,7]. The studies showed that it can cause toxic effects even though at ultra-low-concentration of  $\mu\text{g L}^{-1}$  (part per billion) [8]. As a result, the World Health Organization (WHO) recommends  $1 \mu\text{g L}^{-1}$  as the maximum concentration of total mercury in drinking water [9]. Therefore, removing trace mercury from the natural water is an urgent matter.

At present, many methods have been developed to remove mercury in water, such as chemical coagulation [10], adsorption [11], electrocoagulation [12] and membrane filtration [13]. Among them, the adsorption method could be a practical and economic method compared to other techniques because of its

comparatively low cost, high efficiency, simplicity of operation and lower secondary pollution [14]. Multiple sorbents have been widely investigated to capture mercury from wastewater, including zeolites [15], activated carbons [16], metal oxidize [17] and nanocellulose [18]. However, such materials usually face challenges with relatively low adsorption capacities, low surface area and moderate affinity for mercury [19]. The main mechanism of them were physisorption, which results in low adsorption capacity due to the weak binding ability. Therefore, exploring a stable, large surface area and effective adsorbent for removal of mercury ions is of considerable importance.

Metal organic frameworks (MOFs) are composed of organic ligands and metal ions or clusters with infinite network, which are new type of microporous and mesoporous materials. MOFs have advantages of high porosity, diversity in structure, large specific surface area, relatively easy modification, chemistry and thermal stability, etc [20]. The network topology, shape and pore size of the material can be controlled by selecting different metal ions and organic ligands to achieve specific applications. Because of the advantages proposed above, MOFs are widely used in gas storage [21], adsorption [22], separation [23,24], catalysis [25] and fluorescence sensing [26]. In recent years, the research on the removal and adsorption of heavy metal pollutants from aqueous environment by MOFs is attracting attentions [27–30]. For example, an ethylenediamine-functionalized MIL-101-Cr was used

to adsorb  $\text{Pb}^{2+}$  in lake and river water samples [31], the results revealed that the sorbent could reduce the lead concentrations to as low as  $0.3\text{--}0.5\text{ mg L}^{-1}$  from  $10\text{ mg L}^{-1}$ . So far, most of the researches are mainly about removal of heavy metal pollutants at comparable higher  $\text{mg L}^{-1}$  concentrations, but effective removal of heavy metal pollutions at  $\mu\text{g L}^{-1}$  levels is still a challenge [32]. The absorption performance of trace  $\text{Hg}^{2+}$  was detected by using unmodified MOF-74-Zn material and the removal efficiency of 57.08%, 54.48% and 72.26% were obtained at  $45^\circ\text{C}$  when its concentrations were at  $10\text{ }\mu\text{g L}^{-1}$ ,  $20\text{ }\mu\text{g L}^{-1}$  and  $50\text{ }\mu\text{g L}^{-1}$ , respectively [33]. However, it is still a big challenge to reduce the residual  $\text{Hg}^{2+}$  to below  $1\text{ }\mu\text{g L}^{-1}$  in solution. This is due to the lack of strong binding capacity among metal ions and action sites which hinders the capture of metal ions.

(Dresden University of Technology) DUT-67 (Zr) was a water and acidic stable metal-organic framework with the composition of  $[\text{Zr}_6\text{O}_6(\text{OH})_2(\text{tdc})_4(\text{CH}_3\text{COO})_2]$  [34], which had large specific surface area, the ligand of thiophene aromatic had a S element and could be a potential candidate for dealing with heavy metals in water. In this work, DUT-67 (Zr) was synthesized and used as an adsorbent to remove trace mercury and methylmercury ions in water. The factors that affected absorption performance including contact time, pH and temperature were studied and the influence of humic acid (HA) was also investigated. Finally, we applied it to remove the trace mercury and methylmercury ions in the water samples and achieved satisfactory results.

## 2. Experimental

### 2.1 Chemicals and materials

In this experiment, the solvents and reagents without further purification were commercially available. Zirconium chloride was purchased from Macklin Biochemical Co., Ltd. (Shanghai, China). 2, 5-thiophenedicarboxylic acid ( $\text{H}_2\text{tdc}$ ) was from J&K Scientific Ltd. (Beijing, China). N-methyl pyrrolidone (NMP), acetic acid and N, N-dimethylformamide (DMF) were purchased from Fuchen Chemical Reagents Factory (Tianjin, China). Ethanol was purchased from Beijing Chemical Works (Beijing, China). KOH (GR Grade) and NaOH (purity,  $\geq 96\%$ ) were obtained from Sinopharm Chemical Reagent Co., Ltd. (Shanghai, China).  $\text{KBH}_4$  (purity,  $\geq 98.5\%$ ) was obtained from Tianjin Institute of Fine Chemicals (Tianjin, China).  $65\% \text{ HNO}_3$  was purchased from Merck KGaA (Darmstadt, Germany). Stock standard solution of mercury ( $1000\text{ mg L}^{-1}$ ) and methylmercury ( $69.5\text{ mg L}^{-1}$ ) were obtained from Putian Tongchuang Biotechnology Co., Ltd. (Beijing, China). Milli-Q Advantage A10 system (Millipore, Molsheim, France) was applied to make ultrapure water.

### 2.2. Instruments

The Bruker D8-Focus Bragg-Brentano X-ray powder diffractometer was used to measure the X-ray diffraction (XRD) pattern of DUT-67 (Zr), which is equipped with a Cu sealed tube ( $\lambda = 1.54178$ ). Scanning electron microscope (SEM) image was measured at  $15.0\text{ KV}$  on a Shimadzu SS-550 scanning electron microscope. The TGA-50 (SHIMADZU) thermogravimetric analyzer was used to obtain Thermal gravimetric analysis (TGA) image of DUT-67 (Zr) with a heating rate of  $10^\circ\text{C min}^{-1}$  under a  $\text{N}_2$  atmosphere. Under  $\text{N}_2$  absorption at  $77\text{ K}$ , the BET of DUT-67 (Zr) was obtained on a Micromeritics ASAP2020 surface area. The concentration of mercury was detected on an AFS-8130 atomic fluorescence spectrometer equipped with a flow injection system.

### 2.3. Preparation of DUT-67 (Zr) and characterization

The DUT-67 (Zr) was synthesized according to the reported method [34]. A solid mixture of  $\text{H}_2\text{tdc}$  ( $220\text{ mg}$ ,  $1.34\text{ mmol}$ ) and Zirconium chloride ( $460\text{ mg}$ ,  $2\text{ mmol}$ ) were dissolved in DMF ( $25\text{ mL}$ ) and NMP ( $25\text{ mL}$ ) by sonication for  $10\text{ min}$ . After that acetic acid ( $14\text{ mL}$ ,  $234\text{ mmol}$ ) was added to the solution and sonicated for  $10\text{ min}$ . The resulting solution was then transferred into a Teflon lining stainless steel reaction kettle and heated up to  $120^\circ\text{C}$  for  $48\text{ h}$ . The resulted powder was separated by centrifugation and washed once with DMF and then ethanol for the second time. Afterwards, it was dried at  $80^\circ\text{C}$  for  $2\text{ h}$ . The XRD, TGA, SEM and  $\text{N}_2$  adsorption-desorption experiments were used to analyze the synthesized of DUT-67 (Zr)

### 2.4. Removal and determination of $\text{Hg}^{2+}$ and $\text{CH}_3\text{Hg}^+$

Considering of the concentration of mercury ions in water environment is usually around  $\mu\text{g L}^{-1}$  of magnitudes, we chose  $20\text{ }\mu\text{g L}^{-1}$  as the experimental concentration. The effects of varying pH and temperature were studied at a pH range of  $2\text{--}7$  and temperature range of  $15^\circ\text{C}\text{--}55^\circ\text{C}$ , respectively, we keep the sample  $10\text{ mg}$  of DUT-67 (Zr) was added to  $10\text{ mL}$  of  $20\text{ }\mu\text{g L}^{-1}$   $\text{Hg}^{2+}$  and  $\text{CH}_3\text{Hg}^+$  solution.  $\text{HNO}_3$  and NaOH were to adjust the pH of the solution. In order to study the kinetic rules of the absorption, approximately  $10\text{ mg}$  of DUT-67 (Zr) was immersed in  $50\text{ mL}$  of  $50\text{ }\mu\text{g L}^{-1}$   $\text{Hg}^{2+}$  and  $\text{CH}_3\text{Hg}^+$  solution with continuous stirring. The concentrations of  $\text{Hg}^{2+}$  and  $\text{CH}_3\text{Hg}^+$  in  $2\text{ mL}$  supernatant were measured by AFS when it was removed from the solutions at every set time. To determine the effect of HA in the adsorption process, a batch adsorption experiment of varying concentrations of HA from  $0$  to  $2\text{ mg L}^{-1}$  were also

studied. Finally, the adsorption of  $\text{Hg}^{2+}$  and  $\text{CH}_3\text{Hg}^+$  by DUT-67 (Zr) in real water samples were evaluated.

The DUT-67 (Zr) was separated from the solution by filtration, the solution was diluted and concentrated  $\text{HNO}_3$  was added to the volume of 10 mL and  $\text{HNO}_3$  concentration was about 2% (v/v). Then the concentrations of  $\text{Hg}^{2+}$  and  $\text{CH}_3\text{Hg}^+$  in the solution were measured by AFS. The mobile phase were A: 2%  $\text{KBH}_4$  (m/v) in 0.5%  $\text{KOH}$  (m/v) and B: 2%  $\text{HNO}_3$  (v/v). The sample, phase A and phase B were mixed firstly and then went through the atomizer. The  $\text{Hg}^{2+}$  and  $\text{CH}_3\text{Hg}^+$  was analyzed on-line reducing before cold vapor generation. Table 1 lists the specific experimental conditions about the atomic fluorescence spectrometer (CV-AFS). Each sample in this work were detected three times and took the average.

The removal efficiency (R) of the mercury and the amount of mercury adsorbed by the unit mass adsorbent were calculated by Equations (1) and (2):

$$R(\%) = \frac{c_0 - c_e}{c_0} \times 100\% \quad (1)$$

$$q = \frac{c_0 - c_e}{m} \times V \quad (2)$$

In the above formulas, the initial and equilibrated concentrations of mercury are expressed in  $c_0$  ( $\text{mg L}^{-1}$ ) and  $c_e$  ( $\text{mg L}^{-1}$ ), respectively.  $m$  (g) represents the quality of the adsorbent.  $q$  ( $\text{mg g}^{-1}$ ) is the amount adsorbed per gram of adsorbent, and the initial volume of the mercury solution is represented by  $V$  (L).

### 3. Results and discussion

#### 3.1. Characterization of DUT-67 (Zr)

The characteristic XRD pattern of the as-synthesized DUT-67 (Zr) was shown in Figure 1(a). The measured and simulated of diffraction peaks for DUT-67 (Zr) were in good agreement. Thermogravimetric analysis of DUT-67 were shown in Figure 1(b). The first step in the curve shows the loss of mass (28%) was in the range of temperature from 34°C to 100°C, which was associated with the removal of free guest solvent and water molecules in pores. The framework was stable up to 350°C, beyond which the structure would be decomposed. The scanning electron microscope (SEM) image of DUT-67 (Zr) (Figure 1(c)) indicates that it consisted of globular crystallites with an average particle size of about 2.5  $\mu\text{m}$ . The nitrogen sorption-desorption isotherms of the as-synthesized

**Table 1.** CV-AFS conditions for mercury determination.

Parameters	Optimized values
Hollow-Cathode Lamp	Mercury HCL 253.7 nm
Lamp current	30 mA
PMT voltage	-270 V
Argon flow rate	200 mL/min
Atomization temperature	Room temperature
$\text{KBH}_4$ concentration	2% (m/v) in 0.5% $\text{KOH}$ (m/v)
$\text{HNO}_3$ concentration	2% (v/v) in water
Sampling time	10 s
Injection time	25 s
Signal collection time	5 s

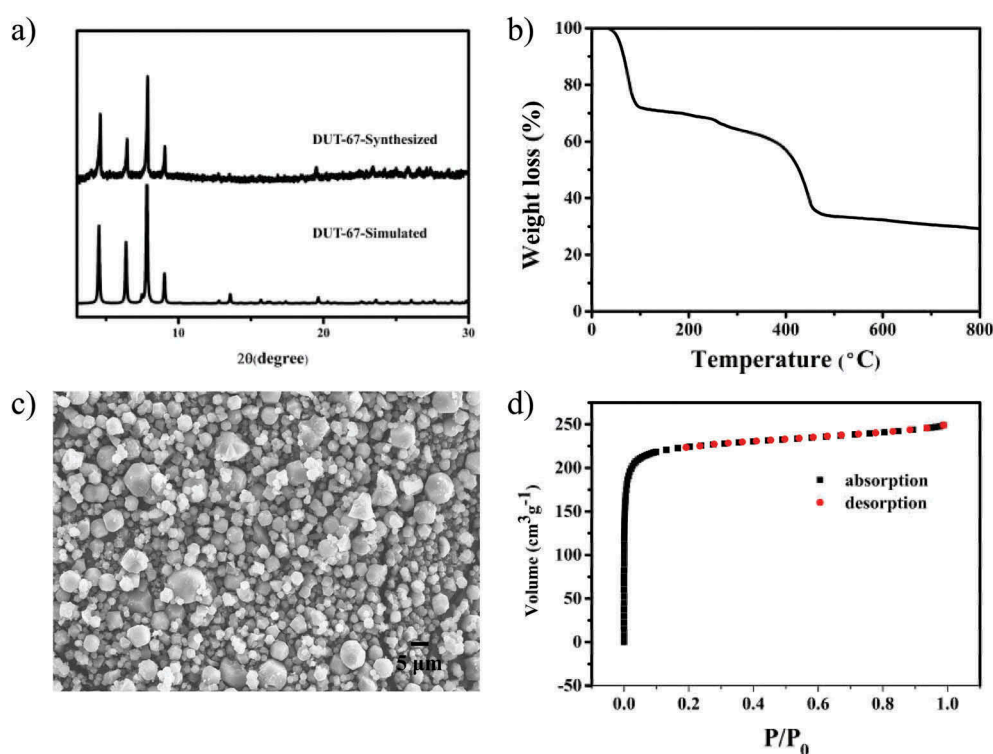


**Figure 1.** (a) XRD of the synthesized DUT-67 (Zr), and the simulated XRD curve. (b) TGA image of the synthesized DUT-67 (Zr). (c) SEM image of the synthesized DUT-67 (Zr). (d) nitrogen sorption-desorption isotherms image of the synthesized DUT-67 (Zr).

sample were measured as well (see Figure 1(d)).  $781.8 \text{ m}^2 \text{ g}^{-1}$  and  $0.3412 \text{ cm}^3 \text{ g}^{-1}$  ( $P/P_0 = 0.2$ ) were the total pore volume and surface area of the adsorption, respectively. The average diameter of the pore was  $1.766 \text{ nm}$ , which indicated that the synthesized DUT-67 (Zr) was one kind of micro-pore material.

### 3.2. Effect of pH on adsorption

The effect of pH on the adsorption of DUT-67 (Zr) is of great importance due to the different forms of  $\text{Hg}^{2+}$  and  $\text{CH}_3\text{Hg}^+$  at different pH. When the pH of the aqueous solution is lower than 3, mercury ions exist as  $\text{Hg}^{2+}$ . However, when the solution pH higher than 6,  $\text{Hg}(\text{OH})_2$  is its dominant form. When pH between 3 and 6, three kinds of forms co-exist, including  $\text{Hg}^{2+}$ ,  $\text{Hg}(\text{OH})_2$ ,  $\text{Hg}(\text{OH})^+$  [35]. For methylmercury, the main form in the acid condition is  $\text{CH}_3\text{Hg}^+$ . With the increase of pH, the  $\text{CH}_3\text{Hg}^+$ ,  $(\text{CH}_3\text{Hg})_2\text{OH}^+$  and  $\text{CH}_3\text{HgOH}$  may co-exist in the solution. However, under alkaline conditions ( $\text{pH} > 8$ ),  $\text{CH}_3\text{HgOH}$  is the main form of existence [36]. To select the best pH of adsorption, the adsorption behavior of  $\text{Hg}^{2+}$  and  $\text{CH}_3\text{Hg}^+$  on DUT-67 (Zr) were investigated at the pH range of 2–7. The results were shown in Figure 2. The results showed that there was a relatively lower removal efficiency of  $\text{Hg}^{2+}$  at the low pH condition, and as the pH increasing, the adsorption efficiency of  $\text{Hg}^{2+}$  was significantly increased and reached the maximum value when  $\text{pH} = 6$ . This results was mainly caused by the protonation of the active sites of DUT-67 (Zr) under the lower pH. The protonation of active sites of DUT-67 (Zr) decreased with the pH increases and the active sites became more beneficial for sorption of  $\text{Hg}^{2+}$  to DUT-67 (Zr). When the  $\text{pH} > 6$ , the adsorption efficiency of  $\text{Hg}^{2+}$  decreased due to the hydrolysis of metal ion and it competed the metal ion adsorption on DUT-67 (Zr). However, the change of

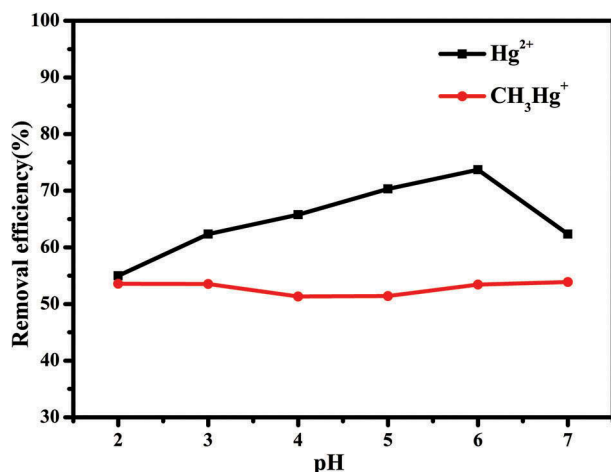


**Figure 2.** The removal efficiency of DUT-67 (Zr) for  $\text{Hg}^{2+}$  and  $\text{CH}_3\text{Hg}^+$  at different pH.  $c_0 = 20 \text{ ppb}$ ,  $V = 10 \text{ mL}$ ,  $m = 10 \text{ mg}$ ,  $t = 2 \text{ h}$ ,  $T = 25^\circ\text{C}$ .

pH value did not have obvious effect on the adsorption of  $\text{CH}_3\text{Hg}^+$ . Thus, the pH 6 was chosen in the subsequent adsorption experiments.

The aperture size of DUT-67 (Zr) was about  $14.2 \text{ \AA}$  and  $11.7 \text{ \AA}$  [34], which is large enough for  $\text{Hg}^{2+}$  ( $2.2 \text{ \AA}$ ) [37],  $\text{Hg}(\text{OH})^+$  and  $\text{Hg}(\text{OH})_2$  ( $8.22 \text{ \AA}$ ) [38]. Meanwhile, the size of  $\text{CH}_3\text{Hg}^+$  was about  $4 \text{ \AA}$  which can also be passed through the hole [39]. According to the structural features, the ligand of S-heterocyclic aromatic compound coordinate with mercury species, and there could be slight  $\pi$ -complexation between thiophene ring of DUT-67 (Zr) and  $\text{Hg}^{2+}$ .

### 3.3. Effect of temperature and thermodynamic parameters

The adsorption of  $\text{Hg}^{2+}$  and  $\text{CH}_3\text{Hg}^+$  by DUT-67 (Zr) were observed by varying the adsorption temperature from  $15^\circ\text{C}$  to  $55^\circ\text{C}$  (see Figure 3). With the increase of the temperature from  $15^\circ\text{C}$  to  $55^\circ\text{C}$ , the removal efficiency of  $\text{Hg}^{2+}$  and  $\text{CH}_3\text{Hg}^+$  increased from 47% to 65% and from 42% to 55%, respectively. The increase of removal efficiency with temperature increase implies that the adsorption could be an endothermic process, which meant there may be chemical adsorption exist, such as the ligand of S-heterocyclic aromatic compound coordinate with mercury species and the  $\pi$ -complexation between thiophene ring of DUT-67 (Zr) and  $\text{Hg}^{2+}$ . Accordingly, the value of  $55^\circ\text{C}$  was selected as the optimum temperature in the subsequent adsorption experiments.

Furthermore, the Gibbs free energy of adsorption ( $\Delta G$ ,  $\text{kJ} \cdot \text{mol}^{-1}$ ), the change of entropy ( $\Delta S$ ,  $\text{J} \cdot \text{mol}^{-1} \cdot \text{K}^{-1}$ ) and the change of enthalpy ( $\Delta H$ ,  $\text{kJ} \cdot \text{mol}^{-1}$ ) as the three basic thermodynamic parameters were calculated by using the following Equation (3), (4) and (5).

$$\Delta G = \Delta H - T\Delta S \quad (3)$$

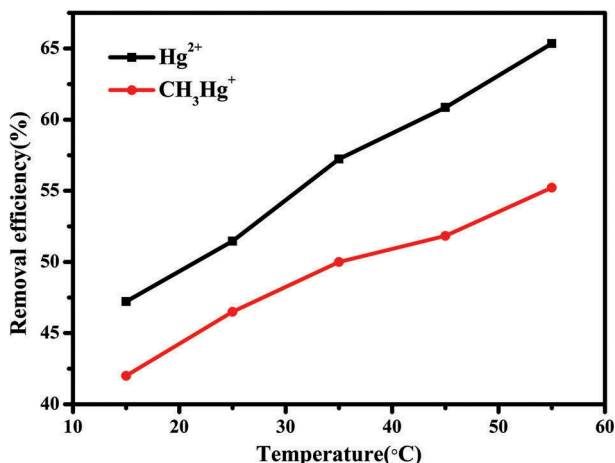


**Figure 3.** The effects of different temperature on the removal efficiency of DUT-67 (Zr) for  $\text{Hg}^{2+}$  and  $\text{CH}_3\text{Hg}^+$ .  $c_0 = 20 \text{ ppb}$ ,  $V = 10 \text{ mL}$ ,  $m = 10 \text{ mg}$ ,  $t = 2 \text{ h}$ ,  $\text{pH} = 6$ .

$$\ln K_d = \frac{\Delta S}{R} - \frac{\Delta H}{RT} \quad (4)$$

$$K_d = \frac{V}{m} \times \frac{c_0 - c_e}{c_e} \quad (5)$$

The changes of Gibbs free energy, enthalpy and entropy are expressed in  $\Delta G$  ( $\text{kJ mol}^{-1}$ ),  $\Delta H$  ( $\text{kJ mol}^{-1}$ ) and  $\Delta S$  ( $\text{J (mol K)}^{-1}$ ), respectively.  $R$  ( $8.314 \text{ J (mol K)}^{-1}$ ) represents the universal gas constant. The distribution coefficient of adsorption is  $K_d$ .  $T$  (K) is the Kelvin temperature. According to the slope and intercept of the plot of  $\ln K_d$  against  $1/T$ , the results of  $\Delta H$  and  $\Delta S$  were obtained respectively. The values of  $\Delta S$ ,  $\Delta H$ , and  $\Delta G$  were shown in Table 2.

The adsorption process was endothermic with the positive value of  $\Delta H$ . The negative value of the  $\Delta G$  for these adsorption curves suggested that the spontaneous process of the adsorption reaction. The positive value of  $\Delta S$  confirmed that during the adsorption process, the degrees of freedom and randomness on the DUT-67 (Zr)-solution interface were enhanced.

### 3.4. Adsorption kinetics

The adsorption kinetics was investigated to obtain the adsorption rate at the optimized pH (= 6) and temperature ( $55^\circ\text{C}$ ) (Figure 4). The result revealed that the adsorption rate rapidly increased during the first 20 minutes and then increased slowly. The adsorptive equilibrium was obtained within 1 h.

The pseudo-first-order and pseudo-second-order model was used to evaluate the effect of the contact time, which was shown as Equation (6) and (7), respectively.

$$\ln(q_e - q_t) = \ln q_e - k_1 t \quad (6)$$

$$\frac{t}{q_t} = \frac{1}{k_2 q_e^2} + \frac{t}{q_e} \quad (7)$$

The adsorption capacity are defined as  $q_e$  ( $\text{mg g}^{-1}$ ) and  $q_t$  ( $\text{mg g}^{-1}$ ) at equilibrium and time  $t$ , respectively.  $k_1$  ( $\text{min}^{-1}$ ) and  $k_2$  ( $\text{g (mg min)}^{-1}$ ) are the rate constant of the pseudo-first-order kinetic model and pseudo-second-order kinetic model.

Table 3 showed several parameters and the regression coefficient ( $R^2$ ) that were obtained from the kinetic models. As observed in Figure 5 and Table 3, the experimental data were very consistent with the pseudo-second-order

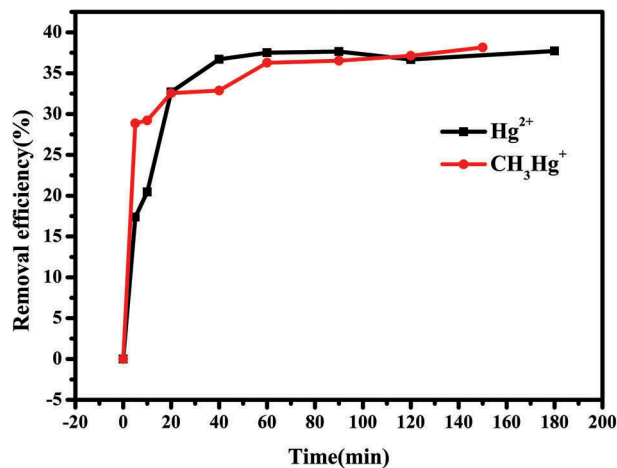


Figure 4. The effects of different contact time on the removal efficiency of DUT-67 (Zr) for  $\text{Hg}^{2+}$  and  $\text{CH}_3\text{Hg}^+$ .  $c_0 = 50$  ppb,  $V = 10$  mL,  $m = 10$  mg,  $\text{pH} = 6$ ,  $T = 25^\circ\text{C}$ .

Table 3. The parameters of the  $\text{Hg}^{2+}$  and  $\text{CH}_3\text{Hg}^+$  adsorption for the kinetic model.

Adsorbate	Kinetics model	Parameter	Quantitative value
$\text{Hg}^{2+}$	Pseudo-first-order	$q_e(\text{exp})$ ( $\text{mg g}^{-1}$ )	0.0451
		$q_e(\text{cal})$ ( $\text{mg g}^{-1}$ )	0.0169
		$k_1$ ( $\text{min}^{-1}$ )	0.0414
		$R^2$	0.5627
	Pseudo-second-order	$q_e(\text{cal})$ ( $\text{mg g}^{-1}$ )	0.0461
$\text{CH}_3\text{Hg}^+$	Pseudo-first-order	$k_2$ ( $\text{g mg}^{-1} \text{min}^{-1}$ )	5.6916
		$R^2$	0.9977
		$q_e(\text{exp})$ ( $\text{mg g}^{-1}$ )	0.0374
		$q_e(\text{cal})$ ( $\text{mg g}^{-1}$ )	0.0135
	Pseudo-second-order	$k_1$ ( $\text{min}^{-1}$ )	0.0244
		$R^2$	0.7939
		$q_e(\text{cal})$ ( $\text{mg g}^{-1}$ )	0.0376
		$k_2$ ( $\text{g mg}^{-1} \text{min}^{-1}$ )	9.0764
		$R^2$	0.9984

kinetic model, and the theoretical values of  $q_e$  ( $0.0461 \text{ mg g}^{-1}$  and  $0.0376 \text{ mg g}^{-1}$  for  $\text{Hg}^{2+}$  and  $\text{CH}_3\text{Hg}^+$ , respectively) obtained from pseudo-second-order kinetic model was very close to the experimental result ( $0.0451 \text{ mg g}^{-1}$  and  $0.0374 \text{ mg g}^{-1}$ ). It was believed that mechanism of physisorption and chemisorption were involved in the current  $\text{Hg}^{2+}$  and  $\text{CH}_3\text{Hg}^+$  adsorption process. According to the structural features, the ligand of S-heterocyclic aromatic compound coordinate with mercury species [40], and act as strong sites for its chemisorption. Meanwhile, there were slight  $\pi$ -complexation between thiophene ring of DUT-67(Zr) and  $\text{Hg}^{2+}$ .

Table 2. The thermodynamics data of  $\text{Hg}^{2+}$  and  $\text{CH}_3\text{Hg}^+$  adsorption onto DUT-67 (Zr).

Adsorbate	$\Delta H^\circ$ ( $\text{kJ mol}^{-1}$ )	$\Delta S^\circ$ ( $\text{J mol}^{-1} \text{K}^{-1}$ )	$\Delta G^\circ$ ( $\text{kJ mol}^{-1}$ )				
$\text{Hg}^{2+}$	14.73	101.76	288.15	298.15	308.15	318.15	328.15
$\text{CH}_3\text{Hg}^+$	10.18	90.23	-14.59	-15.61	-16.63	-17.64	-18.66
			-15.82	-16.72	-17.62	-18.53	-19.43

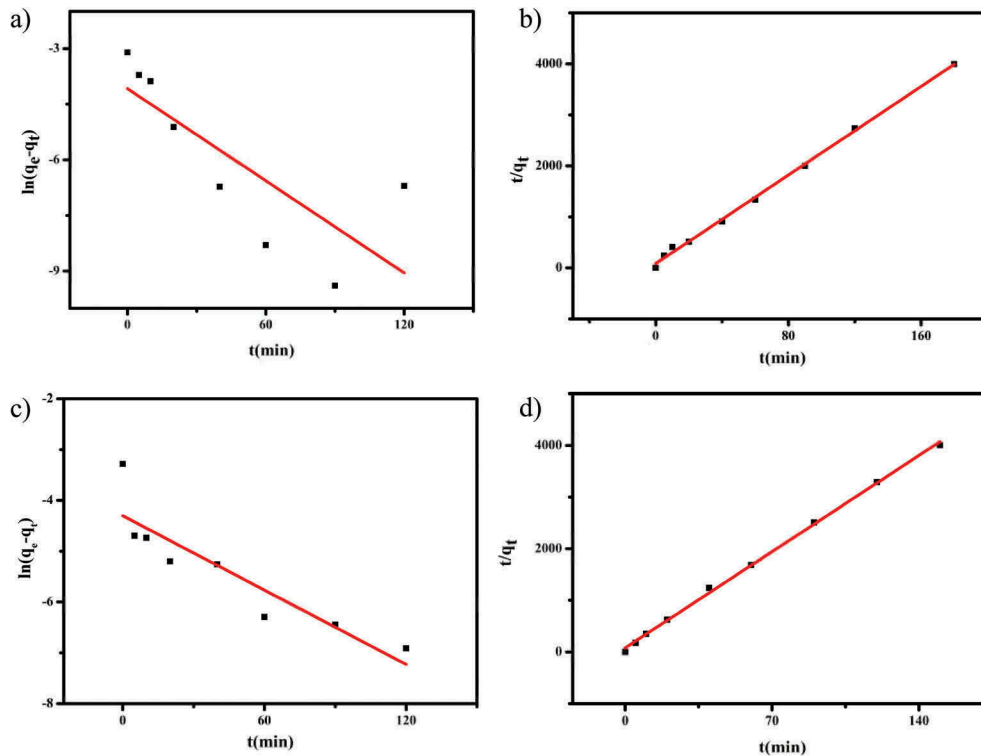


**Figure 5.** (a) Pseudo-first-order adsorption kinetics of  $\text{Hg}^{2+}$  (b) Pseudo-second-order adsorption kinetics of  $\text{Hg}^{2+}$  (c) Pseudo-first-order adsorption kinetics of  $\text{CH}_3\text{Hg}^+$  (d) Pseudo-first-order adsorption kinetics of  $\text{CH}_3\text{Hg}^+$ .

### 3.5. Effect of humic acid on the adsorption of $\text{Hg}^{2+}$ and $\text{CH}_3\text{Hg}^+$

Natural organic matter is a kind of complex material, widely exists in natural and artificial water environment, and plays an important role in the chemical reactions occurring in water environment. A number of studies proved its intramolecular mainly containing carbonyl, carboxyl, hydroxyl, phenolic hydroxyl and other active functional groups, can complex with many organic and inorganic compounds [41]. There are two binding sites with mercury in the natural organic matter, the reduced sulfur is strongly bound to mercury, while carbonyl and phenolic are weakly bound to mercury [42]. It is an important substance that affects DUT-67 (Zr) adsorption of heavy metals in the environment water. It can be seen in Figure 6, as the concentration of HA increased, the adsorption efficiency of  $\text{Hg}^{2+}$  did not changed significantly which could be attributed to the strong attraction of DUT-67 (Zr) towards  $\text{Hg}^{2+}$  than HA. However, the removal efficiency of  $\text{CH}_3\text{Hg}^+$  decreased with the increase of HA concentration. The reason may be there are physisorption and chemisorption between DUT-67 (Zr) and  $\text{Hg}^{2+}$ , but only physisorption adsorption between  $\text{CH}_3\text{Hg}^+$  and DUT-67 (Zr), and the reduced sulfur and carboxyl sites in HA could bind with  $\text{CH}_3\text{Hg}^+$  [43,44]. We tested the infrared spectrum of the DUT-67 (Zr) before and after the adsorption of methyl mercury, but there was no significant change. So, HA in water could reduce the adsorption efficiency of  $\text{CH}_3\text{Hg}^+$ .

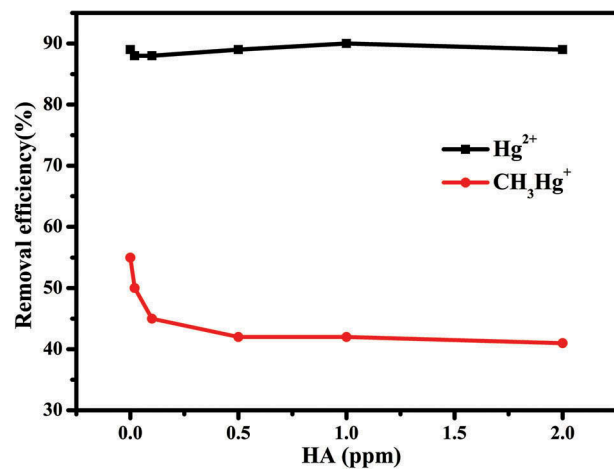


**Figure 6.** The effects of HA on the removal efficiency of DUT-67 (Zr) for  $\text{Hg}^{2+}$  and  $\text{CH}_3\text{Hg}^+$ .  $c_0 = 20$  ppb,  $V = 10$  mL,  $m = 10$  mg,  $\text{pH} = 6$ ,  $T = 25^\circ\text{C}$ .

### 3.6. Removal of $\text{Hg}^{2+}$ and $\text{CH}_3\text{Hg}^+$ with DUT-67 (Zr) in real water samples

The above method was applied to remove the  $\text{Hg}^{2+}$  and  $\text{CH}_3\text{Hg}^+$  in natural water. The results were listed in Table 4. It showed the test water samples contained certain amount of mercury ( $0.67 \mu\text{g L}^{-1}$ ,  $0.51 \mu\text{g L}^{-1}$  for river water and lake water, respectively). The removal efficient of  $\text{Hg}^{2+}$  was more than 90% for all concentrations in natural water, and  $\text{CH}_3\text{Hg}^+$  was 30%-76%. When the concentration of  $\text{Hg}^{2+}$  was

**Table 4.** Adsorption of  $\text{Hg}^{2+}$  and  $\text{CH}_3\text{Hg}^+$  in real water.

Sample	Real sample (total mercury $\mu\text{g/L}$ )	Adsorbate	Added ( $\mu\text{g/L}$ )	Found ( $\mu\text{g/L}$ )	Residual ( $\mu\text{g/L}$ )	Removal efficient (%)
River water	0.67	$\text{Hg}^{2+}$	10	8.8	0.4	95.45
			20	17.96	0.73	95.93
			50	53.78	5.24	90.26
		$\text{CH}_3\text{Hg}^+$	10	11.07	3.31	70.10
			20	22.38	11.09	50.45
			50	49.20	34.20	30.49
Lake water	0.51	$\text{Hg}^{2+}$	10	10.59	0.84	92.07
			20	21.73	0.98	95.49
			50	60.58	4.81	92.06
		$\text{CH}_3\text{Hg}^+$	10	9.07	2.12	76.63
			20	18.28	9.82	46.28
			50	48.61	22.87	52.95

lower than  $20 \mu\text{g L}^{-1}$ , the remaining  $\text{Hg}^{2+}$  levels could reach the standard of WHO ( $1 \mu\text{g L}^{-1}$ ).

#### 4. Conclusions

This study systematically evaluated the removal of  $\text{Hg}^{2+}$  and  $\text{CH}_3\text{Hg}^+$  ions using the synthesized DUT-67 (Zr) from water. The optimum pH value of 6 and temperature ( $55^\circ\text{C}$ ) were selected for  $\text{Hg}^{2+}$  and  $\text{CH}_3\text{Hg}^+$  with the removal efficient of 90% and 55% at  $20 \mu\text{g L}^{-1}$ , respectively. Furthermore, the equilibrium data of  $\text{Hg}^{2+}$  and  $\text{CH}_3\text{Hg}^+$  agreed with pseudo-second order kinetic model. DUT-67 (Zr) was an effective adsorbent for trace  $\text{Hg}^{2+}$  and  $\text{CH}_3\text{Hg}^+$  in natural water, the removal efficiency was about 90% when the concentration of  $\text{Hg}^{2+}$  was lower than  $20 \mu\text{g L}^{-1}$ , and the residual of mercury ions could reach the standard of  $1 \mu\text{g L}^{-1}$  of WHO. There are physisorption, chemisorption between DUT-67 (Zr) and  $\text{Hg}^{2+}$ , the S element in thiophene has a relatively weak adsorption capacity for mercury, and there could be slight  $\pi$ -complexation between thiophene ring of DUT-67 (Zr) and  $\text{Hg}^{2+}$ , while there only was physical adsorption between DUT-67 (Zr) and  $\text{CH}_3\text{Hg}^+$ .

Furthermore, in order to enhance the adsorption capacity for low concentration pollutants, it is feasible scheme to modify the group with strong ability to combine with the target pollutants. For example, thiol-functionalized material was used to remove mercury [45]. At the same time, the anti-interference ability of MOFs should be improved because of the complexity of environmental water. Meanwhile, we need to consider a quick and simple method to separate the adsorbents from environmental water.

#### Acknowledgments

The authors are indebted to Dr. Zhi-Qiang Tan for the detection of samples with the atomic fluorescence spectrometer.

#### Disclosure statement

No potential conflict of interest was reported by the authors.

#### Funding

This work was supported by the National Natural Science Foundation of China [U1407119]; Research Foundation of Beijing University of Technology [005000546318514]

#### References

- [1] Carocci A, Rovito N, Sinicropi MS, et al. Mercury toxicity and neurodegenerative effects. *Rev Environ Contam.* 2014;229:1–18. PubMed PMID: 24515807.
- [2] Rana SVS. Perspectives in endocrine toxicity of heavy metals—a review. *Biol Trace Elem Res.* 2014 Jul;160(1):1–14. PubMed PMID: 24898714.
- [3] Giang A, Stokes LC, Streets DG, et al. Impacts of the minamata convention on mercury emissions and global deposition from coal-fired power generation in Asia. *Environ Sci Technol.* 2015 May 05;49(9):5326–5335. PubMed PMID: 25851589.
- [4] Barkay T, Gillman M, Turner RR. Effects of dissolved organic carbon and salinity on bioavailability of mercury. *Appl Environ Microbiol.* 1997;63(11):4267–4271.
- [5] Rani BK, John SA. Fluorogenic mercury ion sensor based on pyrene-amino mercapto thiadiazole unit. *J Hazard Mater.* 2018 Feb 05;343:98–106.
- [6] Zahir F, Rizwi SJ, Haq SK, et al. Low dose mercury toxicity and human health. *Environ Toxicol Phar.* 2005 Sep;20:351–360. PubMed PMID: 21783611.
- [7] Mondal BC, Das D, Das AK. Application of a new resin functionalised with 6-mercaptopyridine for mercury and silver determination in environmental samples by atomic absorption spectrometry. *Anal Chim Acta.* 2001;450:223–230.
- [8] Boening DW. Ecological effects, transport, and fate of mercury: a general review. *Chemosphere.* 2000;40:1335–1351.
- [9] Zhang FS, Nriagu JO, Itoh H. Mercury removal from water using activated carbons derived from organic sewage sludge. *Water Res.* 2005 Jan-Feb;39:389–395. PubMed PMID: 15644247.
- [10] Lu XX, Huangfu XL, Ma J. Removal of trace mercury(II) from aqueous solution by in situ formed Mn-Fe (hydr) oxides. *J Hazard Mater.* 2014 Sep 15;280:71–78.
- [11] Yee KK, Reimer N, Liu J, et al. Effective mercury sorption by thiol-laced metal-organic frameworks: in strong acid and the vapor phase. *J Am Chem Soc.* 2013 May 29;135(21):7795–7798. PubMed PMID: 23646999.
- [12] Nansau-Njiki CP, Tchamango SR, Ngom PC, et al. Mercury(II) removal from water by electrocoagulation using aluminium and iron electrodes. *J Hazard*



- Mater. 2009 Sep 15;168:1430–1436. PubMed PMID: 19349114.
- [13] Urgun-Demirtas M, Benda PL, Gillenwater PS, et al. Achieving very low mercury levels in refinery wastewater by membrane filtration. *J Hazard Mater.* 2012 May 15;215–216:98–107. PubMed PMID: 22410725.
- [14] Bennett GF. Book reviews. *J Hazard Mater.* 2004;109(1–3):227–229.
- [15] Lopes CB, Lito PF, Otero M, et al. Mercury removal with titanosilicate ETS-4: batch experiments and modelling. *Micro Meso Mater.* 2008;115(1–2):98–105.
- [16] Faulconer EK, Reitzenstein N, Mazyck DW. Optimization of magnetic powdered activated carbon for aqueous Hg(II) removal and magnetic recovery. *J Hazard Mater.* 2012 Jan 15;199–200:9–14.
- [17] Sreepasad TS, Maliyekkal SM, Lisha KP, et al. Reduced graphene oxide-metal/metal oxide composites: facile synthesis and application in water purification. *J Hazard Mater.* 2011 Feb 15;186(1):921–931. PubMed PMID: 21168962.
- [18] Geng B, Wang H, Wu S, et al. Surface-tailored nanocellulose aerogels with thiol-functional moieties for highly efficient and selective removal of Hg(II) ions from water. *ACS Sustainable Chem Eng.* 2017;5(12):11715–11726.
- [19] Liang LF, Chen QH, Jiang FL, et al. In situ large-scale construction of sulfur-functionalized metal-organic framework and its efficient removal of Hg(II) from water. *J Mater Chem A.* 2016;4(40):15370–15374.
- [20] Zhang L, Wang LL, Gong LL, et al. Coumarin-modified microporous-mesoporous Zn-MOF-74 showing ultra-high uptake capacity and photo-switched storage/release of U(VI) ions. *J Hazard Mater.* 2016 Jul 05;311:30–36. PubMed PMID: 26954473.
- [21] Prabhakaran PK, Catoire L, Deschamps J. Aluminium doping composite metal-organic framework by alane nanoconfinement: impact on the room temperature hydrogen uptake. *Micro Meso Mater.* 2017;243:214–220.
- [22] Luo X-P, Fu S-Y, Du Y-M, et al. Adsorption of methylene blue and malachite green from aqueous solution by sulfonic acid group modified MIL-101. *Micro Meso Mater.* 2017;237:268–274.
- [23] Li XX, Shu L, Chen S. Application of metal-organic frameworks in chromatographic separation. *Acta Chim Sinica.* 2016;74(12):969.
- [24] Chen S, Li XX, Shu L, et al. The high efficient separation of divinylbenzene and ethylvinylbenzene isomers using high performance liquid chromatography with Fe-based MILs packed columns. *J Chromatogr A.* 2017 Aug 11;1510:25–32. PubMed PMID: 28662853.
- [25] Yusran Y, Xu D, Fang Q, et al. MOF-derived Co@N-C nanocatalyst for catalytic reduction of 4-nitrophenol to 4-aminophenol. *Micro Meso Mater.* 2017;241:346–354.
- [26] Kumar P, Paul AK, Deep A. Sensitive chemosensing of nitro group containing organophosphate pesticides with MOF-5. *Micro Meso Mater.* 2014;195:60–66.
- [27] Wu Y, Xu G, Liu W, et al. Postsynthetic modification of copper terephthalate metal-organic frameworks and their new application in preparation of samples containing heavy metal ions. *Micro Meso Mater.* 2015;210:110–115.
- [28] Saleem H, Rafique U, Davies RP. Investigations on post-synthetically modified UiO-66-NH<sub>2</sub> for the adsorptive removal of heavy metal ions from aqueous solution. *Micro Meso Mater.* 2016;221:238–244.
- [29] Huang L, He M, Chen B, et al. A mercapto functionalized magnetic Zr-MOF by solvent-assisted ligand exchange for Hg<sup>2+</sup> removal from water. *J Mater Chem A.* 2016;4(14):5159–5166.
- [30] Huang L, He M, Chen B, et al. A designable magnetic MOF composite and facile coordination-based post-synthetic strategy for the enhanced removal of Hg<sup>2+</sup> from water. *J Mater Chem.* 2015;3(21):11587–11595.
- [31] Luo XB, Ding L, Luo JM. Adsorptive removal of Pb(II) ions from aqueous samples with amino-functionalization of metal-organic frameworks MIL-101(Cr). *J Chem Eng Data.* 2015 Jun;60(6):1732–1743. PubMed PMID: WOS:000356316400024.
- [32] Luo F, Chen JL, Dang LL, et al. High-performance Hg<sup>2+</sup> removal from ultra-low-concentration aqueous solution using both acylamide- and hydroxyl-functionalized metal-organic framework. *J Mater Chem A.* 2015;3(18):9616–9620.
- [33] Xiong YY, Li JQ, Gong LL, et al. Using MOF-74 for Hg<sup>2+</sup> removal from ultra-low concentration aqueous solution. *J Solid State Chem.* 2017;246:16–22.
- [34] Bon V, Senkovska L, Baburin LA, et al. Zr- and Hf-Based Metal-organic frameworks: tracking down the polymorphism. *Cryst Growth Des.* 2013;13(3):1231–1237.
- [35] Walcarius A, Delacôte C. Mercury(II) binding to thiol-functionalized mesoporous silicas: critical effect of pH and sorbent properties on capacity and selectivity. *Anal Chim Acta.* 2005;547(1):3–13.
- [36] Sanz J, Raposo JC, Madariaga JM. Potentiometric study of the hydrolysis of (CH<sub>3</sub>)Hg<sup>+</sup> in NaClO<sub>4</sub>: construction of a thermodynamic model. *Appl Organometal Chem.* 2000;14:499–506.
- [37] Ye MM, Lu ZD, Hu YX, et al. Mesoporous titanate-based cation exchanger for efficient removal of metal cations. *J Mater Chem A.* 2013;1(16):5097.
- [38] Tossell JA. Theoretical studies on the formation of mercury complexes in solution and the dissolution and reactions of cinnabar. *Am Mineral.* 1999;84:877–883.
- [39] Jia J, Xu F, Long Z, et al. Metal-organic framework MIL-53(Fe) for highly selective and ultrasensitive direct sensing of MeHg<sup>+</sup>. *Chem Communications.* 2013 May 21;49(41):4670–4672. PubMed PMID: 23586077.
- [40] Wang KK, Huang HL, Xue WJ, et al. An ultrastable Zr metal-organic framework with a thiophene-type ligand containing methyl groups. *CrystEngComm.* 2015;17(19):3586–3590.
- [41] Jones MN, Bryan ND. Colloidal properties of humic substances. *Adv Colloid Interfac.* 1998;78:1–48.
- [42] Drexel RT, Haitze M. Mercury(II) sorption to two Florida everglades peats: evidence for strong and weak binding and competition by dissolved organic matter released from the peat. *Environ Sci Technol.* 2002;36:4058–4064.
- [43] Qian J, Skyllberg U. Bonding of methyl mercury to reduced sulfur groups in soil and stream organic matter as determined by x-ray absorption spectroscopy and binding affinity studies. *Geochim Cosmochim Acta.* 2002;66(22):3873–3885.
- [44] Yoon SJ, Diener LM, Bloom PR, et al. X-ray absorption studies of CH<sub>3</sub>Hg<sup>+</sup>-binding sites in humic substances. *Geochim Cosmochim Acta.* 2005;69(5):1111–1121.
- [45] Huang L, Peng C, Cheng Q, et al. Thiol-functionalized magnetic porous organic polymers for highly efficient removal of mercury. *Ind Eng Chem Res.* 2017;56(46):13696–13703.